

# Supplementary Information

## Towards membrane-electrode-assembly systems for CO<sub>2</sub> reduction: a modeling perspective

---

Lien-Chun Weng,<sup>1,2</sup> Alexis T. Bell,<sup>\*1,2</sup> and Adam Z. Weber<sup>\*1</sup>

<sup>1</sup>Joint Center for Artificial Photosynthesis, LBNL, Berkeley CA 94720

<sup>2</sup>Dept. Chemical and Biomolecular Engineering, University of California, Berkeley CA 94720

### First-order approximation of applied voltage breakdown reported in Figure 2

The cathode overpotential for the planar cell is obtained from experimental data reported by Hatsukade et al. of CO<sub>2</sub>R on a planar Ag foil.<sup>1</sup> The cathode overpotential for the GDEs (aqueous GDE, full-MEA, exchange-MEA) is obtained from our previous theoretical calculations,<sup>2</sup> but can also be obtained from experimental data. The anode overpotential is approximated using a Butler-Volmer expression for OER on IrO<sub>2</sub>,

$$i_{OER} = i_{o,OER} \left( \exp \left( \frac{\alpha_a^{OER} F \eta_{OER}}{RT} \right) - \exp \left( - \frac{\alpha_c^{OER} F \eta_{OER}}{RT} \right) \right)$$

where  $i_{o,OER} = 1.4 \times 10^{-4} \text{ mA cm}^{-2}$ ,  $\alpha_a^{OER} = 1$ ,  $\alpha_c^{OER} = 0.1$ .<sup>3</sup> The anode overpotentials calculated this way deviate slightly ( $< 0.1 \text{ V}$ ) from the OER overpotential reported in **Figure 3** because this Butler-Volmer equation does not include pH-dependent exchange current densities discussed in Eq. (35). The ohmic potentials are calculated using Ohm's law with the assumed conductivities ( $6 \text{ S m}^{-1}$  for  $0.5 \text{ M KHCO}_3$ , and  $0.5 \text{ S m}^{-1}$  for the membrane). The distance between the anode and cathode is assumed to be  $1 \text{ cm}$  for the aqueous planar and aqueous GDE cells, and  $50 \mu\text{m}$  for the MEAs. This is a quick-and-dirty way to obtain voltage breakdowns for an electrochemical cell, and does not take into account various ion and water transport effects, temperature effects, etc.

### Ionic limitation in the cathode catalyst layer for a full-MEA

CO<sub>2</sub> concentration remains relatively constant throughout the CL at total current densities up to  $1 \text{ A cm}^{-2}$  (**Figure S1a**), indicating that the full-MEA is not limited by CO<sub>2</sub> mass transport. However, the local CO

partial current density shifts towards the membrane/CL boundary as the total current density increases (Figure S1b). This is because, as the membrane dries out, the CL ionic conductivity drops, causing the electrolyte potential gradient to increase (Figure S1c & d).

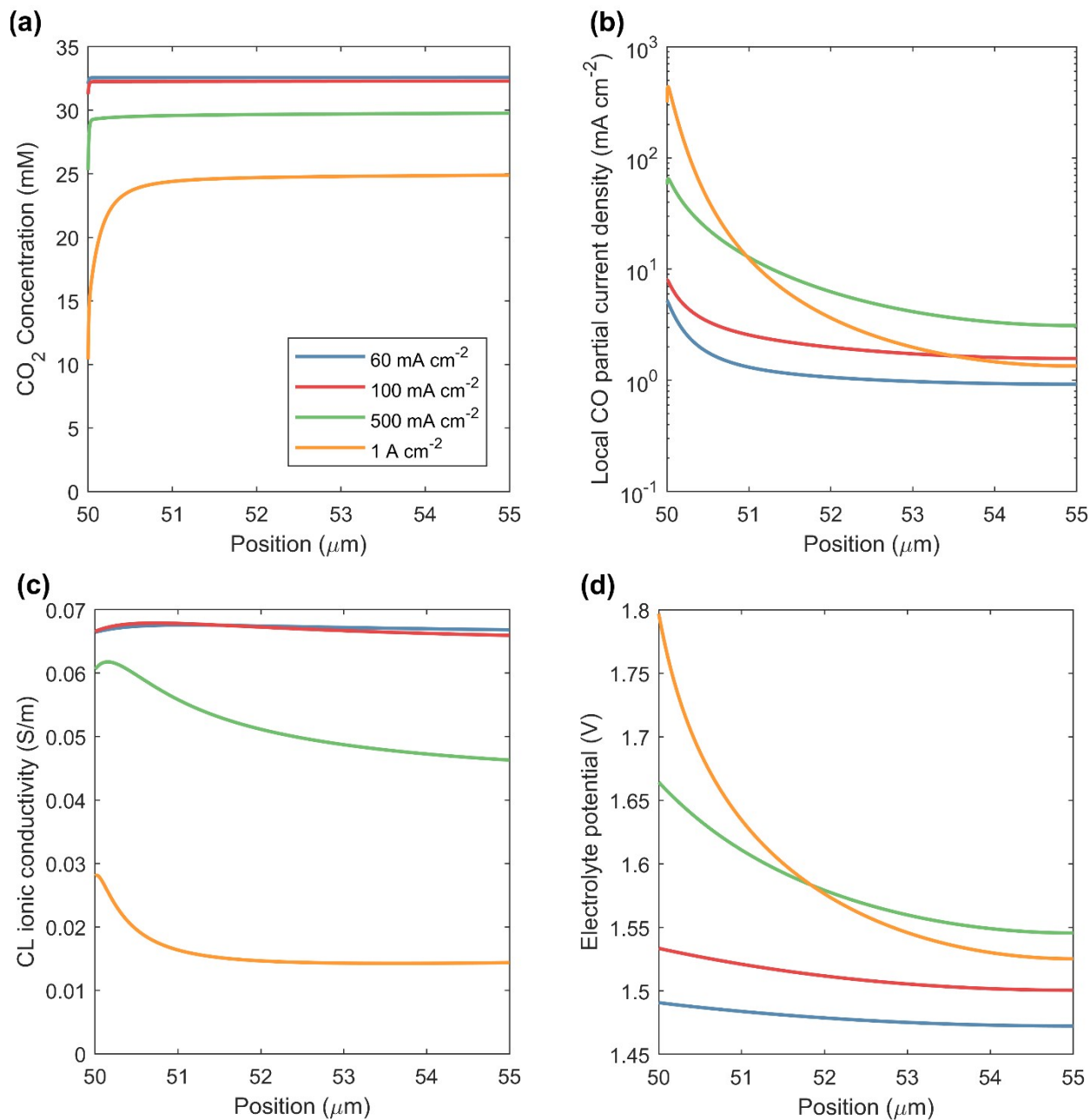


**Figure S1** (a) CO<sub>2</sub> concentration profile within the CL at various current densities showing the full-MEA is not limited by CO<sub>2</sub> mass transport. (b) Local CO partial current density shifts towards the membrane/CL boundary (position at 50 μm) as the total current density increases. (c) The CL ionic conductivity decreases significantly as total current density increases. (d) Electrolyte potential gradient within the CL increases as the CL becomes less ionically conductive.

## Increasing CO<sub>2</sub> utilization

The CO<sub>2</sub> utilization efficiency is dependent on the rate of CO<sub>2</sub> consumption by OH<sup>-</sup> relative to that of the electrochemical conversion of CO<sub>2</sub> to CO. The forward rate constant of the homogeneous reaction,  $CO_2 + OH^- \leftrightarrow HCO_3^-$ , has been reported to range from 10<sup>3</sup> ~ 10<sup>5</sup> L mol<sup>-1</sup> s<sup>-1</sup>. The model assumes a value of 10<sup>3</sup> L mol<sup>-1</sup> s<sup>-1</sup> for  $k_3$ . Here, we show the how the CO<sub>2</sub> utilization can efficiency can be increased if we were to slow down the reaction between CO<sub>2</sub> and OH<sup>-</sup> (**Figure S2**). The curve for  $k_3 = 10^3$  L mol<sup>-1</sup> s<sup>-1</sup> overlaps with that for  $k_3 = 10^4$  L mol<sup>-1</sup> s<sup>-1</sup>, governed by the stoichiometric balance shown in **Figure 7**. This suggests that impeding homogeneous reactions without affecting electrochemical reactions should be a design target for ionomers used in CO<sub>2</sub>R electrolyzers.

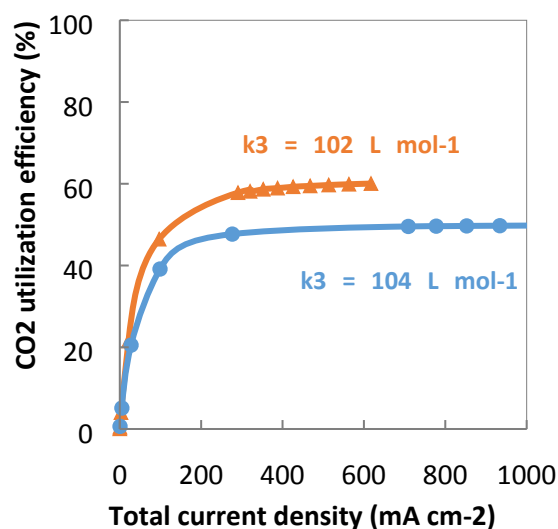


**Figure S2** Utilization vs TCD for rate constants an order of magnitude lower than used (orange) and an order of magnitude higher than used (blue). Slower CO<sub>2</sub> consumption by OH<sup>-</sup> increases the CO<sub>2</sub> utilization efficiency.

## Sensitivity analysis

### Electro-osmotic coefficient

While the electro-osmotic drag (EOD) coefficient has been reported to be higher for a KOH-equilibrated AEM, our model shows minimal dependence of the KOH exchange-MEA's performance on the EOD coefficient. Therefore, we use a value of one for all our scenarios.

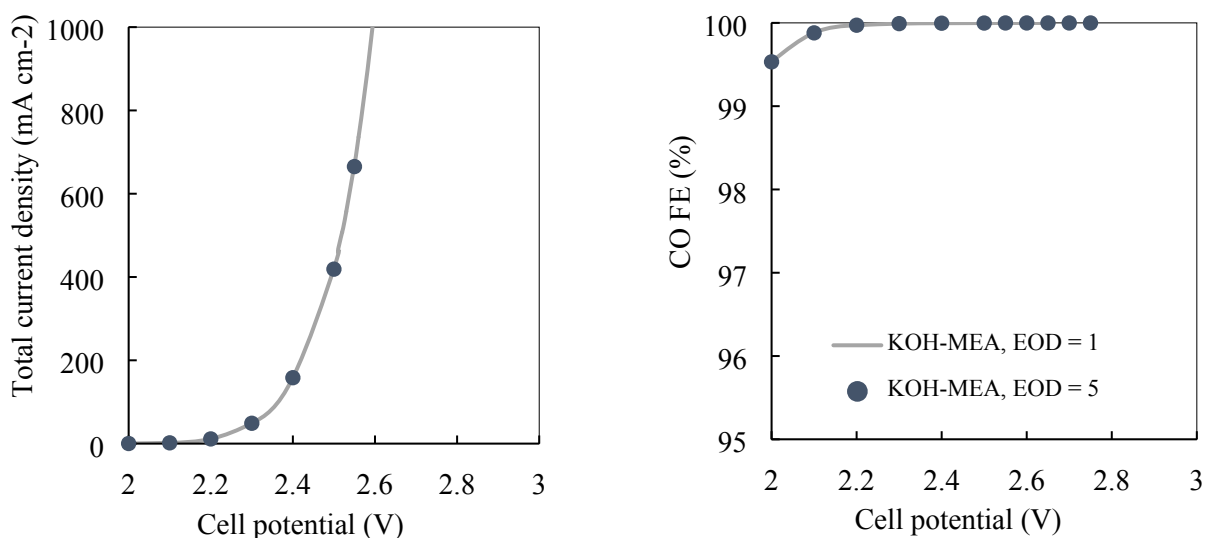


**Figure S3** (a) Total current density and (b) CO faradaic efficiency for the KOH-MEA case simulated with two electro-osmotic coefficients. Simulation results show that the model is insensitive to the coefficient value.

### CO<sub>2</sub> reduction kinetic parameters

We performed a sensitivity study on the exchange current density for COER,  $i_{o,COER}$ , by simulating the full-MEA performance with  $0.1 \times i_{o,COER}$  and  $10 \times i_{o,COER}$ , essentially increasing/decreasing the apparent activation energy for COER,  $E_{a,COER}$ , by 0.059 eV. An order-of-magnitude increase in  $i_{o,COER}$  improves the TCD by approximately 30 mA cm<sup>-2</sup> at cell potentials > 3 V, and lowers the cell potential needed to achieve > 99% CO FE by about 150 mV (**Figure S4**). This minimal change in the TCD at > 3 V cell potentials confirms our finding that the system is ohmic limited at high TCDs (**Figure 3**). In contrast, the CO partial current density varies almost proportionally with  $i_{o,COER}$  at 2V (**Figure S4c**), which is when the cell is kinetically limited.

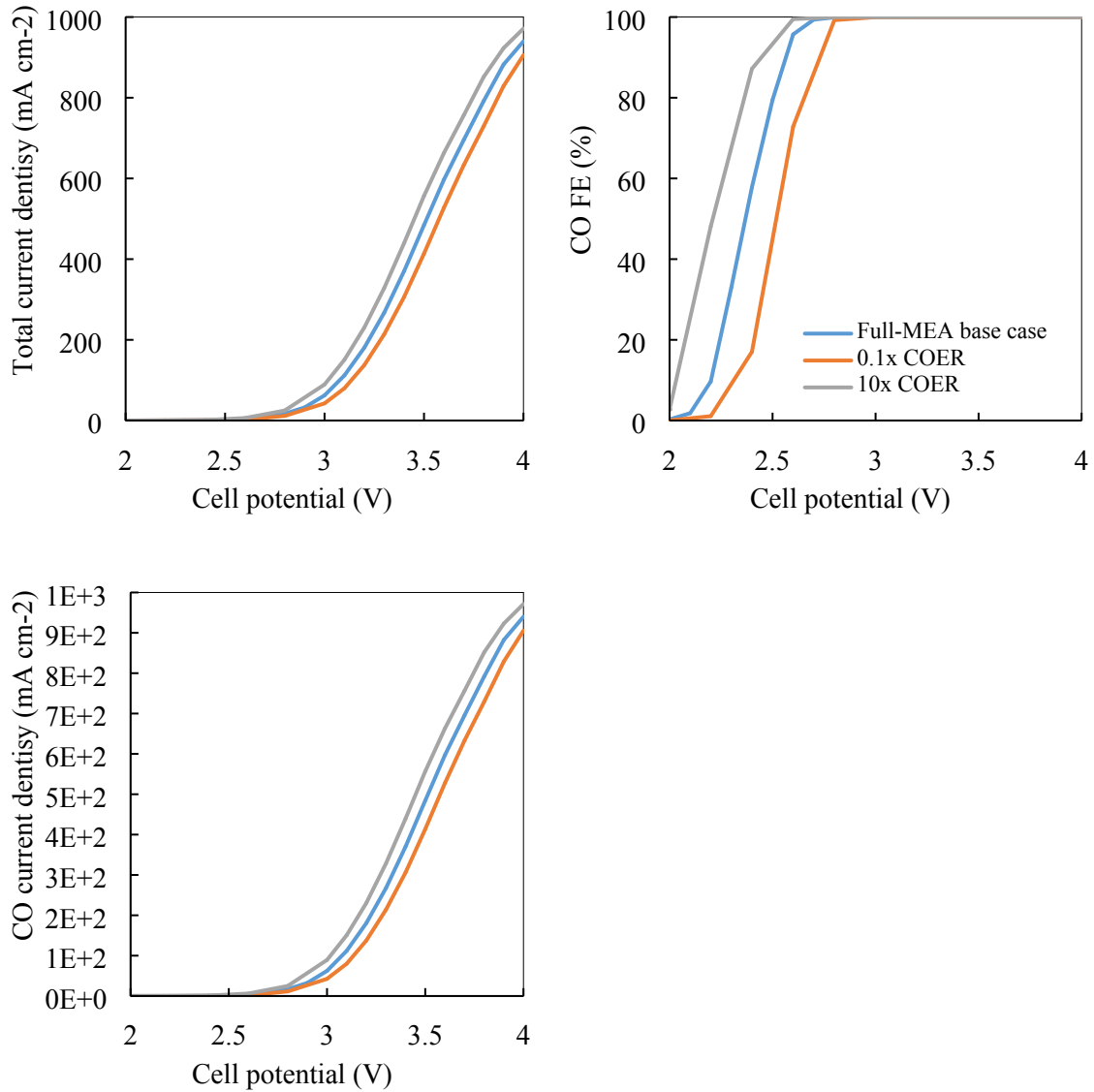


**Figure S4** (a) Total current density, (b) CO faradaic efficiency, (c) CO partial current density for the full-MEA case simulated with an exchange CO current density a magnitude lower (orange) and a magnitude higher (grey) than the base case (blue). Simulation results indicate that the MEA is not kinetically limited at high cell potentials.

### Membrane properties

To study the effects of temperature-sensitive water sorption membranes, we modified our isotherm to include a temperature-dependent term such that the water content increases one unit for every five-

degree increase in temperature, i.e.  $\lambda = f_{T_o}(a_w) + \frac{1}{5}(T - T_o)$  where  $f_{T_o}$  is the temperature-independent isotherm we used in our original model.

Figure S4 shows that an AEM with a temperature-dependent water-uptake isotherm slightly improves the full-MEA performance, as can be expected. The temperature of the full-MEA increases during operating due to processes such as ohmic heating, improving water uptake and minimizing dehydration issues we see in our base case model (Figure 5). These results suggest the importance of water management of our system, and the possibility of leveraging temperature increase of these systems to enhance water-uptake of the ionic membranes.

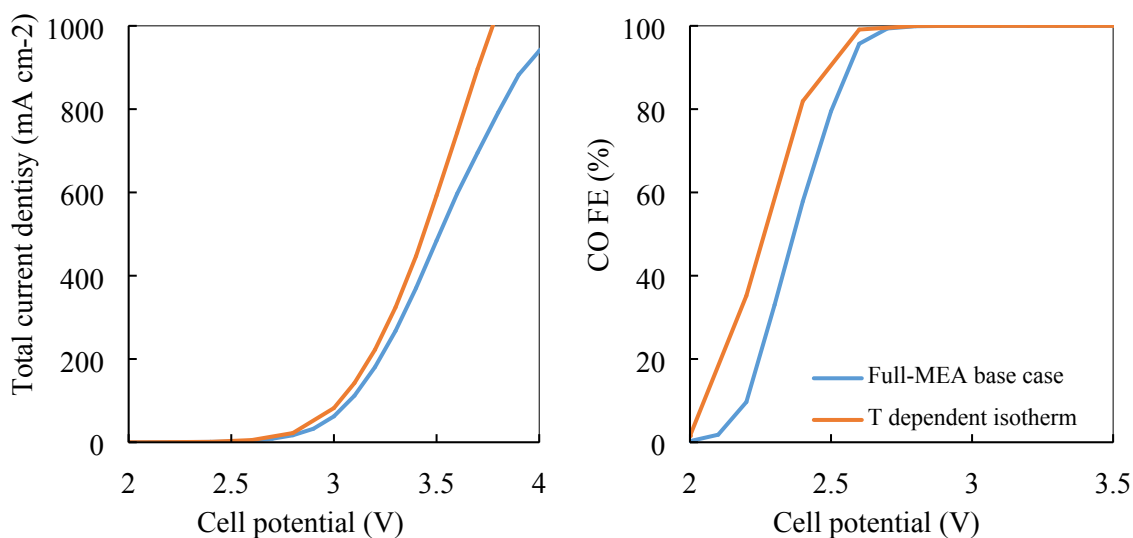


**Figure S5** (a) Total current density and (b) CO faradaic efficiency for the full-MEA case with a membrane that has a temperature-independent water-uptake isotherm (Full-MEA base case, blue), or temperature-dependent one (orange).

## References

1. T. Hatsukade, K. P. Kuhl, E. R. Cave, D. N. Abram and T. F. Jaramillo, *Phys. Chem. Chem. Phys.*, 2014, **16**, 13814-13819.
2. L. C. Weng, A. T. Bell and A. Z. Weber, *Phys. Chem. Chem. Phys.*, 2018, **20**, 16973-16984.
3. C. C. McCrory, S. Jung, J. C. Peters and T. F. Jaramillo, *J. Am. Chem. Soc.*, 2013, **135**, 16977-16987.